Photochemical Core Manipulation in High-Nuclearity Os-Hg Clusters

L. H. Gade,[†] B. F. G. Johnson,[†] J. Lewis,*[,†] M. McPartlin,*[,‡] T. Kotch,[§] and A. J. Lees*[,§]

Contribution from the University Chemical Laboratory, Lensfield Road, Cambridge CB2 1EW, U.K., School of Chemistry, The Polytechnic of North London, Holloway Road, London N7 8DB, U.K., and Department of Chemistry, State University of New York at Binghamton, P.O. Box 6000, Binghamton, New York 13902-6000. *Received March 21, 1991*

Abstract: The cluster dianion $[Os_{18}Hg_3C_2(CO)_{42}]^{2-}$ (**2**) has been synthesized in over 90% yield by reacting $[Os_{10}C(CO)_{24}]^{2-}$ with 1.6 equiv of $Hg(O_2CCF_3)_2$, and the molecular structure of its $[PPN]^+$ salt ($[PPN]^+$ = bis(triphenylphosphine)iminium(1+)) was determined by X-ray crystallography. The cluster contains a central Hg_3 triangle fusing two tricapped-octahedral Os_9 fragments together: triclinic, $P\bar{1}$, a = 19.022 (4) Å, b = 15.737 (3) Å, c = 15.204 (3) Å, α = 115.66 (2)°, β = 68.32 (2)°, γ = 115.45 (3)°, V = 3612.2 Å^3, Z = 1, R = 0.0859. **2** undergoes partial demercuration on irradiation with visible light to generate the corresponding dimercury cluster dianion $[Os_{18}Hg_2C_2(CO)_{42}]^{2-}$ (**3**), which thermally reincorporates metallic mercury quantitatively, thus making **2** a photochromic system. The structure of **3** contains a dimercury fragment sandwiched between the two Os_9 subclusters in a uniquely compact way. Both dianions **2** and **3** can be reversibly oxidized to their corresponding monoanions that are related to each other by a similar reversible photochemical process. Quantum yields for the photolytic Hg extrusion for both systems were obtained from spectral sequences after successive irradiation with the 458-, 488-, and 514-nm lines of an Ar ion laser. They lie between 0.004 and 0.006 for the dianionic and between 0.003 and 0.005 for the monoanionic cluster, reflecting the efficiency of nonreactive deactivation pathways in these systems. Irradiation with UV light at 337 nm (N_2 laser) favors the competing CO dissociation leading to a drop in the quantum efficiency of the demercuration by an order of magnitude.

There is an ever growing number of structurally characterized high-nuclearity clusters containing more than ten metal atoms,[1] while their chemical behavior, especially the manipulation of their metal core, remains almost unexplored. An underlying problem inhibiting the systematic investigation of their reactivity is the delicate balance between their metal-metal and metal-ligand bond structures which, if disrupted, may lead to more or less complete disintegration of the system. A way out of this dilemma is the buildup of cluster structures in which the metal core is locally labilized, i.e. activated only with respect to certain metal-metal bond cleavages, thereby allowing specific structural modifications under appropriate reaction conditions. Mixed-metal clusters containing late transition or main group metal atoms with significantly different electronic properties from those of the principal core metal meet these requirements. The resultant polar metal-metal bonds are potentially intrinsic sites of chemical or even photochemical reactivity.

We have recently synthesized and studied a number of Os-Hg clusters derived from reactions of the cluster dianion $[Os_{10}C(CO)_{24}]^{2-}$ (**1**) with a range of different mercury electrophiles.[2] Through careful selection of the solution properties of the Hg reagents the generation of a variety of novel structural types, containing up to 21 metal atoms, was achieved. On going, for example, from the highly dissociated salt $Hg(O_3SCF_3)_2$ to the corresponding trifluoroacetate and by modification of the stoichiometry a complete change of the reaction pathway was effected. While the former generated the Hg-linked cluster $[\{Os_{10}C(CO)_{24}\}_2Hg]^{2-}$ in good yields (eq 1) the latter yielded the cluster $[Os_{18}Hg_3C_2(CO)_{42}]^{2-}$ (**2**) very selectively (eq 2). The full details

$$2[PPN]_2[Os_{10}C(CO)_{24}] + Hg(O_3SCF_3)_2 \rightarrow [PPN]_2[\{Os_{10}C(CO)_{24}\}_2Hg] + 2[PPN][O_3SCF_3] \quad (1)$$

$$2[PPN]_2[Os_{10}C(CO)_{24}] + 3Hg(O_2CCF_3)_2 \rightarrow [PPN]_2[Os_{18}Hg_3C_2(CO)_{42}] + 2[PPN][Os(CO)_3(O_2CCF_3)_3] \quad (2)$$

of the structure of the monomercury-linked dianion and of other mercury-containing products, specifically obtained by appropriately tuning the reagents and reaction conditions, are being published separately.[2b] The octadecaosmium-trimercury cluster **2** contains a triangular Hg_3 subunit, sandwiched between two tricapped-octahedral $Os_9C(CO)_{21}$ fragments derived from **1** by removal of a capping $Os(CO)_3$ vertex (Figure 1).[3] The system has clearcut interfaces between the different metallic domains and therefore, in the context of the strategy outlined above, appeared to be the ideal model system for reactivity studies specifically involving the metal core.

The observation of the light sensitivity of **2** in solution was the starting point for a systematic study of its photolysis and the related chemistry.[4] Photochemically induced reactions affecting either the metal core or ligand shell of high-nuclearity clusters are almost unexplored. Research in this field has so far focussed on trinuclear and, to a lesser extent, tetranuclear systems with specific emphasis on ligand activation and substitution.[5,6] Here

[†] University Chemical Laboratory.
[‡] The Polytechic of North London.
[§] State University of New York at Binghamton.

(1) Representative examples: (a) Chini, P. *J. Organomet. Chem.* **1980**, *200*, 37. (b) Martinengo, S.; Sironi, A.; Chini, P. *J. Am. Chem. Soc.* **1978**, *100*, 7076. (c) Ciani, G.; Magni, A.; Sironi, A.; Martinengo, S. *J. Chem. Soc., Chem. Commun.* **1981**, 1280. (d) Martinengo, S.; Ciani, G.; Sironi, A. *J. Am. Chem. Soc.* **1980**, *102*, 7564. (e) Jackson, P. F.; Johnson, B. F. G.; Lewis, J.; Nelson, W. J. H.; McPartlin, M. *J. Chem. Soc., Dalton Trans.* **1982**, 2099. (f) Ceriotti, A.; Demartin, F.; Longoni, G.; Manassero, M.; Marchioni, M.; Piva, G.; Sansoni, M. *Angew. Chem., Int. Ed. Engl.* **1985**, *24*, 697. (g) Fenske, D.; Ohmer, J.; Hachgenei, J. *Angew. Chem., Int. Ed. Engl.* **1985**, *24*, 993. (h) Ceriotti, A.; Fait, A.; Longoni, G.; Piro, G.; Demartin, F.; Manassero, M.; Masciocchi, N.; Sansoni, M. *J. Am. Chem. Soc.* **1986**, *108*, 8091. (i) Mednikov, E. G.; Eremenkov, N. K.; Slovokhotov, Y. L.; Struchkov, Y. T. *J. Chem. Soc., Chem. Commun.* **1987**, 218. (j) Teo, B. K.; Hong, M. C.; Zhang, H.; Huang, D. B. *Angew. Chem., Int. Ed. Engl.* **1987**, *26*, 897. (k) Charalambous, E.; Gade, L. H.; Johnson, B. F. G.; Lewis, J.; McPartlin, M.; Powell, H. R. *J. Chem. Soc., Chem. Commun.* **1990**, 688. (l) Amoroso, A. J.; Gade, L. H.; Johnson, B. F. G.; Lewis, J.; Raithby, P. R.; Wong, W. T. *Angew. Chem., Int. Ed. Engl.* **1991**, *30*, 107.

(2) (a) Gade, L. H.; Johnson, B. F. G.; Lewis, J.; McPartlin, M.; Powell, H. R. *J. Chem. Soc., Chem. Commun.* **1990**, 110. (b) Gade, L. H.; Johnson, B. F. G.; Lewis, J.; McPartlin, M.; Morris, J.; Powell, H. R. *J. Chem. Soc., Dalton Trans.* Submitted for publication.

(3) The Ru analogue has also recently been prepared: Bailey, P. J.; Johnson, B. F. G.; Lewis, J.; McPartlin, M.; Powell, H. R. *J. Chem. Soc., Chem. Commun.* **1989**, 1513. There is, however, at present no indication of a similar photochemical behavior on irradiation with visible light: Bailey, P. J. Personal communication.

(4) Charalambous, E.; Gade, L. H.; Johnson, B. F. G.; Kotch, T.; Lees, A. J.; Lewis, J.; McPartlin, M. *Angew. Chem., Int. Ed. Engl.* **1990**, *29*, 1137.

(5) (a) Gallop, M. A.; Johnson, B. F. G.; Lewis, J.; McCamley, A.; Perutz, R. N. *J. Chem. Soc., Chem. Commun.* **1988**, 1071. (b) Malito, J.; Markiewicz, S.; Poë, A. J. *Inorg. Chem.* **1982**, *21*, 4335. (c) Poë, A. J.; Sekhar, C. V. *J. Am. Chem. Soc.* **1986**, *108*, 3673. (d) Bengtsen, J. G.; Wrighton, M. S. *J. Am. Chem. Soc.* **1987**, *109*, 4518. (e) Bengtsen, J. G.; Wrighton, M. S. *J. Am. Chem. Soc.* **1987**, *109*, 4530. (f) Desrosiers, M. F.; Wink, D. A.; Trautman, R.; Friedmann, A. E.; Ford, P. C. *J. Am. Chem. Soc.* **1986**, *108*, 1917.

0002-7863/91/1513-8698$02.50/0

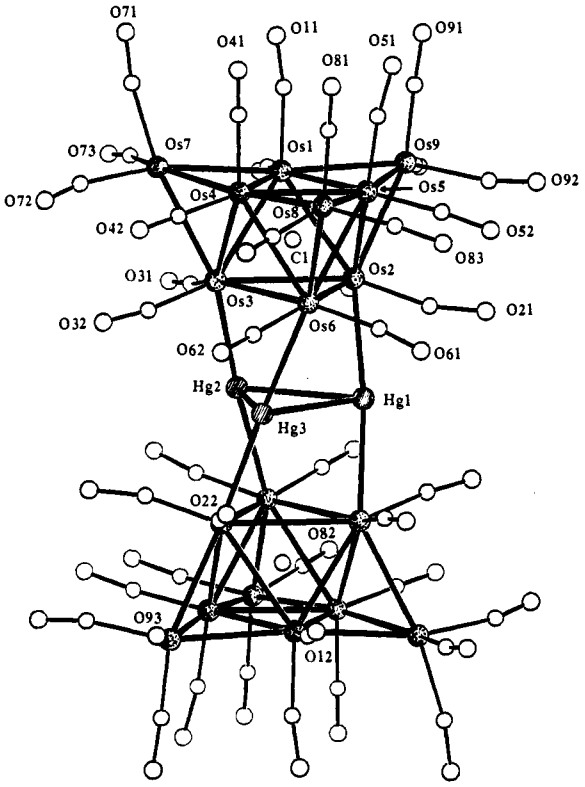

Figure 1. The molecular structure of the cluster dianion in **2**. For clarity all atoms are drawn as spheres of arbitrary radius; the oxygen and carbon atoms of each CO group have the same number.

we present the syntheses of $[Os_{18}Hg_3C_2(CO)_{42}]^{2-}$ (**2**) and its photolysis product $[Os_{18}Hg_2C_2(CO)_{42}]^{2-}$ (**3**) and a detailed photochemical investigation of the reaction leading to **3**. Full details of the X-ray crystal structure of the $[PPN]^+$ salt of **2** are reported. A preliminary report of the strucutre analysis of the $[PPN]^+$ salt of the dimercury cluster **3**, which suffers from disorder, has already been published;[4] so far it has proved impossible to obtain better crystals of **3**.

Experimental Section

Preparation of Compounds. All manipulations were performed under an inert gas atmosphere of dried argon in standard (Schlenk) glassware. $[PPN]_2[Os_{10}C(CO)_{24}]$ ($[PPN]^+$ = bis(triphenylphosphine)iminium(1+)) was prepared as reported in the literature.[1e] All other chemicals were obtained commercially and used without further purification. Dichloromethane used in the syntheses was dried over CaH_2, distilled, and saturated with argon or N_2 before use. The ^{13}C-enriched samples used for the ^{13}C NMR studies reported in this paper were synthesized from ^{13}C-enriched $Os_3(CO)_{12}$. The enrichment of the osmium carbonyl was achieved as follows: Finely powdered $Os_3(CO)_{12}$ (1.5 g) was suspended in 60–70 mL of dry toluene in a 250-mL carius tube with an attached Young tap. The solvent was degassed by three successive freeze–pump–thaw cycles and then pressurised to 1 atm with ^{13}CO (97–99%). The suspension was heated at 130 °C (at which temperature all the $Os_3(CO)_{12}$ dissolved) in the closed tube for 3 days. The solution was then cooled down to room temperature and the solvent evaporated under vacuum. The enriched $Os_3(CO)_{12}$ was obtained as a yellow microcrystalline solid. The enrichment in ^{13}CO achieved in a single cycle was ca. 30% as determined by mass spectroscopy. A second cycle yielded an ~50% enriched product.

$[PPN]_2[Os_{18}Hg_3C_2(CO)_{42}]$ (2). *Note: The synthesis of this compound was carried out under rigorous exclusion of light!* **1** (500 mg, 0.1365 mmol) was dissolved in CH_2Cl_2 (40 mL) and solid $Hg(O_2CCF_3)_2$ (94 mg, 0.2184 mmol = 1.6 equiv) added to the solution. After being stirred for 1 h the solvent volume was reduced to ca. 25 mL and the reaction mixture was left standing at room temperature for seven days and then stored at −25 °C overnight. Within this period 368 mg (85%) of pure $[PPN]_2[Os_{18}Hg_3C_2(CO)_{42}]$ precipitated which was isolated by removal of the liquor with a cannula. The remaining solution was evaporated to dryness, and the residue extracted twice with methanol and recrystallized from dichloromethane–diethyl ether to yield a further 38 mg of **2**. Total yield: 403 mg (93%). Anal. Calcd for $C_{116}H_{60}P_4N_2Os_{18}Hg_3$: C, 22.09; H, 0.95; N, 0.44. Found: C, 22.01; H, 0.94; N, 0.46. IR(CH_2Cl_2) ν 2072 (m), 2057 (s), 2005 (s). ^{13}C NMR (62.8 MHz, 50% ^{13}C-enriched sample, recorded in CD_2Cl_2 at 295 K) δ = 185.7 (6 CO), 184.9 (6 CO), 177.7 (12 CO, $^2J(^{199}Hg^{13}C)$ = 56 Hz), 175.6 (18 CO), 397.4 (interstitial carbide). The most abundant isotopomers for the cluster anions in the negative ion FAB mass spectrum (NBA matrix) were the following: dianion m/z 2615 (stimulated 2615), monoanion m/z 5228 (simulated 5230). Absorption spectrum (CH_2Cl_2) λ_{max} = 540 nm. The combined methanol extracts were evaporated to dryness to yield $[PPN][Os(CO)_3(O_2CCF_3)_3]$ as a beige powder. IR(CH_2Cl_2) ν(CO) 2127 (s), 2038 (br, vs). ^{13}C NMR (100.6 MHz, CD_2Cl_2) δ = 167.5 (CO), 162.0 (O–$COCF_3$, $^2J(^{19}F^{13}C)$ = 37.2 Hz), 114.6 (−CF_3, $^1J(^{19}F^{13}C)$ = 289.2 Hz. Negative ion FAB mass spectrum: 615 $[M]^-$, 587 $[M - CO]^-$, 559 $[M - 2CO]^-$, 474 $[M - CO - CF_3CO_2]^-$, 446 $[M - 2CO - 2CF_3CO_2]^-$.

$[PPN]_2[Os_{18}Hg_2C_2(CO)_{42}]$ (3). A stirred solution of $[PPN]_2[Os_{18}Hg_3C_2(CO)_{42}]$ (50 mg, 0.0082 mmol) in CH_2Cl_2 was irradiated with a 250-W tungsten lamp with the reaction vessel being externally cooled with water. After ca. 10 min, precipitation of metallic mercury was observed, and the reaction was completed after 40–50 min as judged from the IR spectra recorded during the reaction. During this time the color of the solution changed from deep purple to a much less intense burgundy red. After separation of the mercury by filtration the solvent volume was reduced to 15 mL and the product crystallized by slow vapor diffusion with diethyl ether. Black crystals, yield 45.5 mg (92%). Anal. Calcd for $C_{116}H_{60}P_4N_2Os_{18}Hg_2$: C, 22.82; H, 0.98; N, 0.49. Found: C, 23.01; H, 1.17; N, 0.51. IR(CH_2Cl_2) ν(CO) 2064 (s), 2057 (vs), 2007 (s). ^{13}C NMR (100.6 MHz, 50% ^{13}C-enriched sample, recorded in CD_2Cl_2 at 295 K) δ = 185.8 (6 CO), 185.7 (6 CO), 179.7 (12 CO, $^2J(^{199}Hg^{13}C)$ not resolved), 176.0 (18 CO), 411.1 (interstitial carbide). The most abundant isotopomers for the cluster anions in the negative ion FAB mass spectrum (NBA matrix) were the following: dianion m/z 2514 (simulated 2514.5), monoanion m/z 5028 (simulated 5029). Absorption spectrum (CH_2Cl_2) λ_{max} = 550 nm.

Reinsertion of Metallic Mercury into 3. $[PPN]_2$·**3** (20 mg), prepared as described above, was dissolved in 10 mL of CH_2Cl_2 and one small drop (ca. 10 mg) of mercury metal was added to the system. Rapid stirring in the dark led to complete regeneration of **2** within a period of up to 4 h as judged by IR spectroscopy. A similar experiment was carried out with ^{13}C-enriched species, and the quantitative regeneration of **2** was confirmed by ^{13}C NMR spectroscopy. If the experiment is carried out in a more polar solvent than CH_2Cl_2 such as acetone, the reinsertion may remain incomplete (typically 80–90% regeneration of **2** in acetone).

$[PPN][Os_{18}Hg_3C_2(CO)_{42}]$ (6). $[PPN]_2[Os_{18}Hg_3C_2(CO)_{42}]$ (20 mg, 0.0032 mmol) was dissolved in 20 mL of CH_2Cl_2. To this solution solid $Ag(O_2CCF_3)$ (0.8 mg, 0.0036 mmol) was added. Within ca. 30 s the color of the solution changed from purple to brown-red and IR spectroscopy indicated a complete conversion to the monoanion. The compound could be quantitatively precipitated as a black powder on addition of pentane. Anal. Calcd for $C_{80}H_{30}P_4N_2Os_{18}Hg_3$: C, 16.66; H, 0.53; N, 0.25. Found: C, 16.29; H, 0.70; N, 0.34. IR(CH_2Cl_2) ν(CO) 2085 (m), 2072 (s), 2022 (s). Most abundant isotopomer of the molecular ion in the negative ion FAB mass spectrum: m/z 5227 (simulated 5230). Absorption spectrum (CH_2Cl_2) λ_{max} = 526 nm. Exposure of the solution to moist air led to the immediate and complete regeneration of the starting material. For the photolysis sequences the material was not isolated but generated in situ. $[PPN]$·**6** may alternatively be generated by oxidation of $[PPN]_2$·**2** with 1 equiv of $[(4\text{-}BrC_6H_4)_3N][SbCl_6]$ in THF.

$[PPN][Os_{18}Hg_2C_2(CO)_{42}]$ (7). (a) The solution of $[PPN][Os_{18}Hg_3C_2(CO)_{42}]$ prepared as described above was irradiated with a 250-W tungsten lamp while being cooled by water from the outside of the reaction vessel. Within ca. 40 min the color changed from brown-red to green and IR spectroscopy indicated complete conversion to the dimercury cluster. On exposure to moist air the dianion **3** is generated immediately. The solid compound could be obtained quantitatively by precipitation with pentane. Anal. Calcd for $C_{80}H_{30}P_4N_2Os_{18}Hg_2$: C, 17.25; H, 0.55; N, 0.26. Found: C, 17.03; H, 0.71; N, 0.34. IR(CH_2Cl_2) ν(CO) 2081 (s), 2073 (vs), 2022 (s). Most abundant isotopomer of the molecular ion in the negative ion FAB mass spectrum: m/z 5027 (simulated 5029). Absorption spectrum (CH_2Cl_2) λ_{max} = 570 nm. (b) $[PPN]_2[Os_{18}Hg_2C_2(CO)_{42}]$ (20 mg, 0.0032 mmol) was dissolved in 20 mL of CH_2Cl_2. To this solution solid $Ag(O_2CCF_3)$ (0.8 mg, 0.0036 mmol) was added. The color of the solution changed from burgundy red to green within ca. 1 min, generating the monoanion with the same analytical and spectroscopic properties as above. The solid compound

(6) Bantel, H.; Hansert, B.; Powell, A. K.; Tasi, M.; Vahrenkamp, H. *Angew. Chem., Int. Ed. Engl.* **1989**, *28*, 1059.

Table I. Crystal Data and Experimental Details for **2**

compd	$[N(PPh_3)_2]_2[Os_{18}Hg_3(C)_2(CO)_{42}]\cdot CH_2Cl_2$
formula	$C_{117}H_{62}Cl_2Hg_3N_2O_{42}Os_{18}P_4$
formula wt, amu	6387.65
cell	
a, Å	19.022 (4)
b, Å	15.737 (3)
c, Å	15.205 (3)
V, Å^3	3609.2
α, deg	115.66 (2)
β, deg	68.32 (2)
γ, deg	115.45 (3)
Z	1
temp, K	298
d_{calc}, g/cm^3	2.939
space group	$P\bar{1}$ (No. 2)
crystal shape	irregular
crystal vol. mm^3	0.018
radiation	Mo Kα (λ 0.71069 Å)
μ,[a] cm^{-1}	183.6
scan speed, deg/s	0.50
scan method	$\theta/2\theta$
scan width (θ), deg	0.80
std reflcns[b]	three, scanned every 5 h
θ range, deg	3–25
data collected	$\pm h,\pm k,l$
p factor	0.04
no. of unique data ($F_o^2 \geq 3\sigma(F_o^2)$[c]	4546
no. of parameters[d]	387
R on F_o	0.086
R_w on F_o	0.086

[a] Empirical absorption corrections (see: Walker, N.; Stuart, D. *Acta Crystallogr. Sect. A* **1983**, *39*, 158) were applied in two stages, the first after location of only the metal atoms and their refinement with isotropic thermal parameters. This facilitated location of all non-hydrogen atoms, and after their inclusion, with the H-atoms at idealized positions, the absorption correction procedure was repeated with the original data. [b] Initial studies showed the crystals to decompose rapidly in the X-ray beam apparently due to loss of solvent; in final data collection the crystal was coated with epoxyresin and there was no significant change in the standards. [c] Data collection and processing were by standard methods which have been described previously (see: Jackson, P. F.; Johnson, B. F. G.; Lewis, J.; Nelson, W. J. H.; McPartlin, M. *J. Chem. Soc., Dalton Trans.* **1982**, 2099). [d] Structure solution and refinement was carried out with SHELX76 (g. Sheldrick, Cambridge University. 1976).

could be obtained quantitatively by precipitation with pentane.

X-ray Diffraction Study of $[PPN]_2[Os_{18}Hg_3C_2(CO)_{42}]\cdot CH_2Cl_2$. The preliminary examination of the crystal on a Philips PW1100 four-circle diffractometer indicated the triclinic crystal system, and this was confirmed by Delauney reduction. The unit cell parameters were obtained by least-squares refinement of the setting angles of 25 reflections. The crystal data and experimental details are summarized in Table I.

A Patterson synthesis was solved, assuming the centrosymmetric space group $P\bar{1}$, to give the fractional coordinates of six osmium atoms defining an octahedron. The positions of the remaining metal atoms were located in a subsequent observed-Fourier synthesis showing that each cluster dianion has the metal core of virtual D_3 symmetry shown in Figure 1. There was a 50:50 disorder of the central mercury triangle giving an image of virtual D_{3d} symmetry in the diffraction study with a "Star of David" arrangement of the six half-weight mercury atoms; this may be attributed to a random distribution of the two possible cluster enantiomers throughout the crystal. Close scrutiny of the Patterson synthesis did not distinguish interatomic maxima due to vectors between the two orientations of the Hg_3 triangle; this is inconclusive as to the nature of the disorder due to the very large number of much higher Os···Os vector peaks. Attempts to proceed with the structure determination of the noncentrosymmetric space group $P1$ were precluded by the dominance of the eighteen centrosymmetrically related osmium atoms. All non-hydrogen atoms were located in subsequent difference-Fourier syntheses, and their parameters refined satisfactorily in the centrosymmetric space group. Two maxima, separated by about 3 Å, of approximately half the height expected for chlorine atoms where located outside the bonding range of the dianion and the cations. These were included as chlorine atoms of half occupancy, and a dichloromethane solvate molecule was indicated by the location of a small maximum, assigned as a carbon atom of half occupancy at bonding distance from the two chlorine atoms.

The phenyl rings of the cations were assigned idealized hexagonal geometry (C–C = 1.395 Å and C–H = 0.95 Å) and refined as rigid groups with fixed thermal parameters of 0.10 Å^2 assigned to the hydrogen atoms. In the final stages of full-matrix refinement anisotropic thermal parameters were assigned to the metal and phosphorus atoms and individual weights of $1/\sigma^2(F_o)$ were assigned to each reflection (see Table I). Final positional and isotropic thermal parameters are given in Table II, anisotropic thermal parameters are in Table III, a list of $10F_o$ vs $10F_c$ is given in Table IV, selected bond lengths are listed in Table V, and interbond angles are given in Table VI (all in supplementary material).

Photolysis Experiments. Photolysis experiments at 448, 488, and 514 nm were carried out with a Lexel Corp. Model 95-4 4-W argon ion laser. Typical laser power was in the 25–50-mW range, and the incident light intensities were measured by means of an external Lexel Corp. 504 power meter. Irradiations at 337 nm were performed with a National Research Group, Inc. Model 0.5-5-150B pulsing nitrogen laser calibrated at 5 mJ/pulse with repetition rates of 30–60 pulses/s. In all photolysis experiments the concentrations of reactant and product were monitored throughout the reaction with a Hewlett-Packard 8450A UV–visible spectrophotometer which utilizes a rapid scanning microprocessor-controlled diode array detector. Typically, absorption spectra were obtained from solutions within 5 s of completing the irradiation. Absorption band maxima are considered accurate to ±2 nm in the visible region and ±1 nm in the ultraviolet region. Fourier-transform infrared (FTIR) spectra were also recorded during photolysis on a Nicolet 20 SXC FTIR spectrometer. In the photochemical experiments the sample solutions were prepared in CH_2Cl_2 (HPLC grade) which had been deoxygenated by a freeze–pump–thaw method prior to use. The solutions were filtered through 0.22 μm Milipore films and transferred to a 1-cm quartz cell via an air-tight syringe. During laser photolyses the samples were rapidly stirred to ensure that the solution exhibited homogeneous light absorptions.

Photochemical quantum yields (Φ_{cr}) were determined by monitoring the disappearance of reactant **2** or **6** at their respective visible absorption maxima and by application of eq 3 which accounts for the changing degree of light absorption and for inner-filter effects. Here, [R] is the

$$d[R]/dt = -\Phi_{cr} I_0 (1 - 10^{-D}) \epsilon_R b [R]/D \qquad (3)$$

concentration of the reactant cluster at varying photolysis time t, I_0 is the intensity of the incident light per unit solution volume, ϵ_R and D are the molar extinction coefficients of the reactant cluster and the solution optical density at the photolysis wavelength, respectively, B is the cell path length, and Φ_{cr} is the reaction quantum yield. Plots of $\ln [(D_t - D_\infty)/(D_0 - D_\infty)]$ vs $\int_{t_0}^{t} [(1 - 10^{-D})/D]\, dt$, where D_t, D_∞, and D_0 are the optical densities throughout the photolysis sequence at the reactant's visible absorption maximum, gave straight lines of slope $-\Phi_{cr} I_0 \epsilon_R b$. Quantum yield values were determined in triplicate and found to be within ±8%.

Other Physical Measurements. Infrared spectra were recorded on Perkin-Elmer Models 283B and 1710 FT-IR spectrometers. ^{13}C NMR spectra were recorded on Bruker AM400 and WM250 NMR spectrometers and the negative ion fast atom bombardment mass spectra on a KRATOS MS 50 TC spectrometer (calibrant CsI).

Results and Discussion

Synthesis and Structure of $[PPN]_2[Os_{18}Hg_3C_2(CO)_{42}]$. The reaction of $[PPN]_2[Os_{10}C(CO)_{24}]$ (**1**) with 1.5–1.6 molar equiv of $Hg(O_2CCF_3)_2$ leads to an almost complete conversion to an Os–Hg carbonyl cluster with the stoichiometry $[PPN]_2[Os_{18}Hg_3C_2(CO)_{42}]$ (**2**) and the mononuclear complex $[PPN][Os(CO)_3(O_2CCF_3)_3]$ (**4**) (eq 2). An initial intermediate is the monoanion $[Os_{10}C(CO)_{24}(HgO_2CCF_3)]^-$ (**5**), which, based on the similarity of its IR spectrum to that of the X-ray crystallographically characterized species $[Os_{10}C(CO)_{24}(HgCF_3)]^-$[2a] and $[Os_{10}C(CO)_{24}(HgBr)]^-$,[2b] is thought to have a similar structure with the mercury atom bridging three Os atoms of a capping tetrahedron. The formation of **5** is followed by what appears to be a complicated cascade of reaction steps involving, among others, the nucleophilic attack of $CF_3CO_2^-$ on the activated capping Os atom, as suggested by the nature of the second reaction product **4**. ^{13}C NMR spectroscopic studies of the reaction mixture showed that while **2** is formed within minutes after the addition of the mercury salt, conversions of over 90% are only obtained after reaction times of several days.

The structure of the cluster dianion **2** is illustrated in Figure 1 and principal bond distances are listed in Table V. In the crystal the cluster has virtual D_3 symmetry. The core of 21 metal atoms

Table V. Principal Bond Lengths (Å) for **2**

Os(1)–Os(2)	2.864 (4)	Os(1)–Os(3)	2.867 (3)
Os(1)–Os(4)	2.844 (3)	Os(1)–Os(5)	2.854 (3)
Os(1)–Os(7)	2.773 (3)	Os(1)–Os(9)	2.763 (3)
Os(2)–Os(3)	3.065 (3)	Os(2)–Os(5)	2.857 (4)
Os(2)–Os(6)	3.056 (3)	Os(2)–Os(9)	2.837 (3)
Os(2)–Hg(3)	2.696 (5)	Os(3)–Os(4)	2.877 (3)
Os(3)–Os(6)	3.067 (3)	Os(3)–Os(7)	2.833 (4)
Os(3)–Hg(1)	2.761 (5)	Os(3)–Hg(3)	3.472 (6)
Os(4)–Os(5)	2.844 (3)	Os(4)–Os(6)	2.873 (3)
Os(4)–Os(7)	2.756 (3)	Os(4)–Os(8)	2.746 (3)
Os(5)–Os(6)	2.863 (3)	Os(5)–Os(8)	2.763 (3)
Os(5)–Os(9)	2.755 (3)	Os(6)–Os(8)	2.823 (4)
Os(6)–Hg(2)	2.678 (6)	Hg(1)–Hg(2)	2.931 (6)
Hg(1)–Hg(3)	2.920 (7)	Hg(2)–Hg(3)	2.931 (6)
Os–C (carbonyl) range 1.53 (9)–2.06 (7)			
Os–C (carbide) range 1.95 (5)–2.18 (5)			
C–O range 1.02 (9)–1.29 (7)			

can be divided into three metallic domains: the two tricapped octahedral $Os_9C(CO)_{21}$ fragments, originating from the starting material **1**, and the Hg_3 subcluster which fuses them together. Each Os_9 fragment of the cluster possesses a metal core geometry which until recently has eluded detection in many studies of binary osmium carbonyl systems and, as such, represented a missing link in the structural systematics of these compounds.[7]

The mean twist angle between the central Hg_3 unit and each of the two adjacent Os_3 triangles of 30° results in these faces (Os(2)–Os(3)–Os(6) and Os(2′)–Os(3′)–Os(6′)) of the two Os_9 fragments being staggered with respect to each other. In the crystal the two Os_9 fragments are exactly related by an inversion center, but the overall metal core does not contain this symmetry element due to the arrangement of the mercury atoms. The arrangement of the structural subunits generates a chiral axis through the centers of both Os_9-cluster fragments with a possible left- or righ-handed twist of the central three-metal triangles. The $[PPN]^+$ salt of the cluster crystallizes as a racemic mixture of the two enantiomeric forms randomly distributed throughout the crystal, resulting in a 50:50 disorder of the Hg_3 units.

The most remarkable structural feature of the cluster is the central Hg_3 triangle. The mean Hg–Hg distance of 2.927 (6) Å indicates that the bonding between the mercury centers is rather weak, while their structural significance lies in the linking of the Os_9 subclusters. On the basis of the polyhedral skeletal electron pair theory, an electron count of 122 is required for each Os_9 fragment.[8] Thus, in an extreme approach, a formal tetraanionic charge would be assigned to each nonaosmium moiety, resulting in the formal assignment of the Hg_3 unit as a hexacation. This situation is similar to that in the "raft" cluster $[\{Os_3(CO)_{11}\}_3Hg_3]$,[9] where again all valence electrons of the central Hg_3 triangle are required for each $Os_3(CO)_{11}$ subunit to conform to the 18-electron rule; the mean Hg–Hg distance of 3.100 (3) Å is even longer than that of 2.927 (6) Å in **2**. In both these clusters the Hg–Hg distance does not rule out a mere d^{10}–d^{10} interaction between the Hg(II) centers.[10] Mercury compounds with the same structural arrangement of three Hg atoms, but lower formal charge, show significantly shorter bond lengths, as for instance in the recently described $(Hg_3)^{4+}$ clusters in $Hg_3(dppm)_3(SO_4)_2$ (d = 2.764–2.802 Å)[11] or the mineral terlinguaite, $Hg_4Cl_2O_2$ (2.703 Å).[12] As can

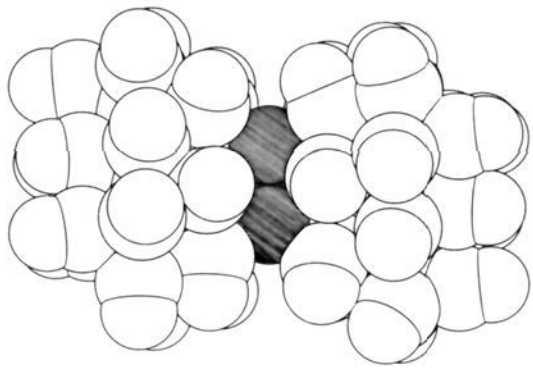

Figure 2. Computed space-filling model of $[Os_{18}Hg_3C_2(CO)_{42}]^{2-}$, showing the exposed situation of the central trimercury unit.

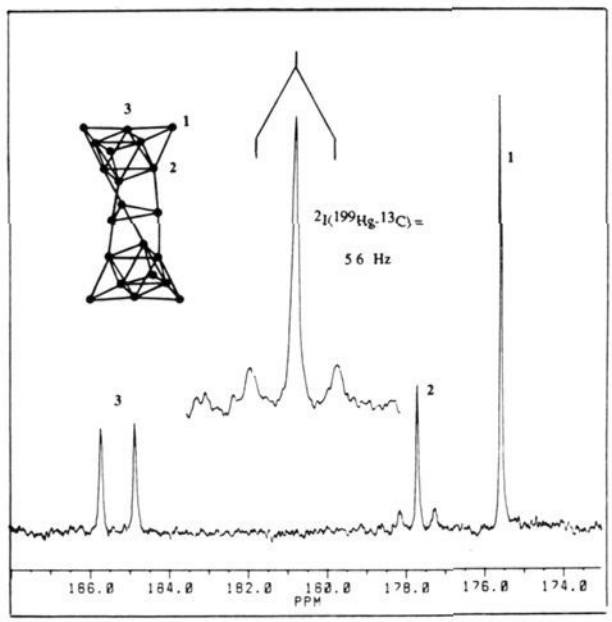

Figure 3. 62.8-MHz ^{13}C NMR spectrum of the 50% ^{13}C-enriched cluster **2** recorded in CD_2Cl_2 at 295 K.

be seen in the computed space filling model in Figure 2, the ligand-free central region of the cluster is remarkably exposed despite slight displacement of the twelve carbonyl ligands adjacent to the mercury unit toward the central triangle which results in a number of short C(carbonyl)···Hg contacts (range 2.559–2.857 Å). The cluster is nevertheless relatively inert with respect to attack by bulky nucleophiles.[13]

The symmetry and ligand distribution of the cluster is reflected in the ^{13}C NMR signal pattern of the 50% ^{13}C-enriched cluster (Figure 3). The four signals due to the carbonyl ligands have an intensity ratio of 1:1:2:3, corresponding to a 6:6:12:18 carbonyls. The most intense signal (δ = 175.6) is the resonance of the $Os(CO)_3$ groups occupying the vertices. As in the case of all high-nuclearity Os and Ru clusters studied so far, there is a fast exchange of the CO's attached to the vertex atoms between the three geometrical positions ("$Os(CO)_3$ rotation") which renders them equivalent on the NMR time scale at ambient temperatures. The signal at δ = 177.7 is due to the 12 CO's coordinated to the two Os_3 triangles adjacent to the central trimercury unit. This assignment is supported by the set of ^{199}Hg satellites associated with the signal. The $^2J(^{199}Hg^{13}C)$ coupling constant of 56 Hz is comparable to the $^2J(^{199}Hg^{13}C)$ observed for $[Ru_4C(CO)_{12}(AuPPh_3)(HgCl)]$ (51 Hz).[14] The two signals at δ = 184.9 and

(7) The cluster dianion $[Os_9(CO)_{24}]^{2-}$ has recently been isolated in very small yields from pyrolysis mixtures and structurally characterized by X-ray crystallography: Amoroso, A. J.; Johnson, B. F. G.; Lewis, J.; Raithby, P. R.; Wong, W.-T. *J. Chem. Soc., Chem. Commun.* **1991**, 814.

(8) (a) Wade, K. In Transition Metal Clusters; Johnson, B. F. G., Ed.; J. Wiley: New York, 1980. (b) Mingos, D. M. P. *Acc. Chem. Res.* **1984**, *17*, 311. (c) McPartlin, M. *Polyhedron* **1984**, *3*, 1279.

(9) Fajardo, M.; Holden, D. H.; Johnson, B. F. G.; Lewis, J.; Raithby, P. R. *J. Chem. Soc., Chem. Commun.* **1984**, 24.

(10) Schmidbaur, H.; Öller, H. J.; Wilkinson, D. L.; Huber, B.; Müller, G. *Chem. Ber.* **1989**, *122*, 31 and references cited therein.

(11) Hämmerle, B.; Müller, E. P.; Wilkinson, D. L.; Müller, G.; Peringer, P. *J. Chem. Soc., Chem. Commun.* **1989**, 1527.

(12) Brodersen, K.; Göbel, G.; Liehr, G. *Z. Anorg. Allg. Chem.* **1989**, *575*, 145.

(13) Another example of a cluster containing a sterically exposed mercury atom has recently been reported: Schoettel, G.; Vittal, J. J.; Puddephatt, R. J. *J. Am. Chem. Soc.* **1990**, *112*, 6400.

(14) Cowie, A. G. Ph.D. Thesis, Cambridge University, 1984.

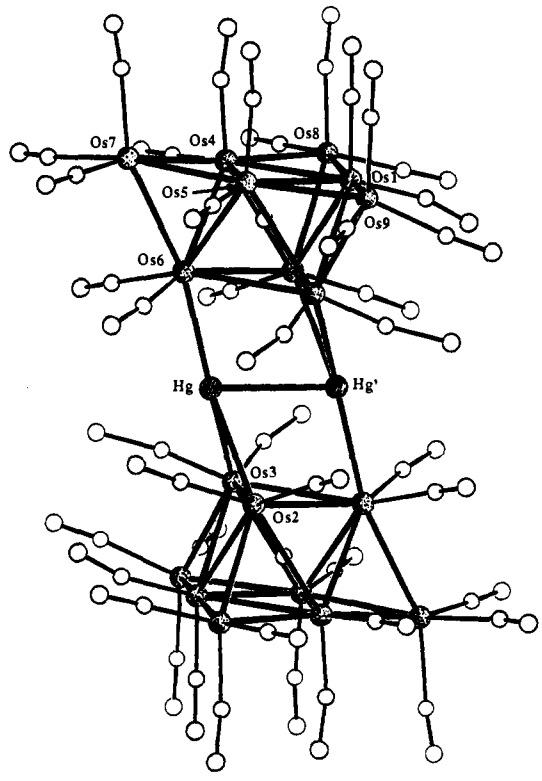

Figure 4. The previously reported structure of the cluster dianion in **3**, redrawn from ref 4, showing the relative "slipping" of the Os_9 subclusters.

185.7 are the resonances of the axial and equatorial carbonyl ligands on the $Os(CO)_2$ fragments in the basal triangles.

Synthesis of $[PPN]_2[Os_{18}Hg_2C_2(CO)_{42}]$ (3). In the course of our investigations into the reactivity of **2**, it was found that when solutions of the cluster were exposed to light their color changed from deep purple to a much less intense burgundy red. Simultaneously, metallic mercury was generated and precipitated. The photochemical reactivity of compounds in which Hg is bound to a transition metal has been known for some time;[15] however, systematic investigations of the reactions occurring are rare.[16] The observation that, on exposure to light, **2** underwent a clean conversion to a single product, **3**, prompted a detailed study of the nature of this process. The light-induced loss of a single Hg atom was confirmed by a negative ion FAB mass spectrum, while the similarity of the IR absorption band patterns of **2** and **3** in the CO-stretching region and the signal pattern in the ^{13}C NMR spectra of both compounds suggested similar overall symmetries. The new cluster, **3**, was thus formulated as $[PPN]_2[Os_{18}Hg_2C_2(CO)_{42}]$.

The molecular structure of **3**, established earlier from X-ray structure analysis of its slightly disordered $[PPN]^+$ salt,[4] is shown in Figure 4. The two nonaosmium subunits already present in **2** remain almost unchanged, but their open Os_3 triangles, while remaining parallel, are markedly "slipped" from the staggered arrangement observed in **2**. Each of the two Hg atoms links an edge of one Os_3 triangle with a corner of the other, generating a hitherto unknown structural environment for a dimercury fragment. The latter is embedded in the metal frame in a uniquely compact way in comparison to other examples of mixed-metal compounds containing Hg_2 units.[17] The reported Hg–Hg distance of 2.744 (5) Å is considerably shorter than the mean Hg–Hg bond length of 2.927 (6) Å in **2**; although the magnitude of this difference indicates a real shortening of the Hg–Hg distance, the observed Hg–Hg length in **3** must be treated with caution due to slight unresolved disorder of the Hg_2 unit.[4]

The photoinduced partial demercuration of **2**, i.e., the extrusion of a single mercury atom, may be viewed as an intramolecular redox reaction in which the remaining core of 20 metal atoms has undergone a formal two-electron oxidation. Thus, **3** is "electron deficient" according to simple electron counting rules, and the slipped structural arrangement of the subclusters, which reduces the perpendicular separation of the open Os_3 triangles by 0.3 Å with respect to **2**, may be a consequence of this electronic situation. This view is supported by the fact that on reduction of **3** to the tetraanion $[Os_{18}Hg_2C_2(CO)_{42}]^{4-}$ the metal core is straightened up again and the separation of the two centroids of the $Os_9C(CO)_{21}$ fragments increased by ca. 0.3 Å.[18]

The ^{13}C NMR spectrum, recorded at 295 K, with its four sharp carbonyl resonances corresponds to a higher symmetry (D_{3h}) with respect to a molecular axis through the centers of both Os units than that displayed in the solid-state structure. We attribute this to a fast rotation of the two Os_9 subclusters relative to each other on the NMR time scale in solution. This interesting observation of core fluxionality is also observed in other high-nuclearity Os–Hg clusters.[19] As in the ^{13}C NMR spectrum for **2** the signal of the interstitial carbide was observed, although significantly shifted to lower field (from δ = 397.4 for **2** to δ = 411.1 for **3**).

If, under exclusion of light, **3** is exposed to metallic mercury, thermal reinsertion of an Hg atom into the metal core occurs, regenerating **2** almost quantitatively within a period of ca. 6–8 h. This process takes place both with the in situ photolytically generated mercury and on addition of mercury to pure **3** isolated previously. The complete thermal reversibility of the photolysis makes **2** the first example of a photochromic high-nuclearity cluster.

Synthesis of the Monoanions $[Os_{18}Hg_3C_2(CO)_{42}]^-$ (6) and $[Os_{18}Hg_2C_2(CO)_{42}]^-$ (7). The dianion **2** may be oxidized by silver salts or other powerful oxidants such as $[(4\text{-}BrC_6H_4)_3N][SbCl_6]$ to the corresponding monoanion $[Os_{18}Hg_3C_2(CO)_{42}]^-$ (**6**) which is stable in solution under an inert gas atmosphere, while on exposure to moist air **2** is regenerated immediately. The CO absorption band pattern in the infrared spectrum of **6** is similar to that of **2** but shifted by ca. 15 cm^{-1} to higher wave numbers, a shift characteristic of a change by one charge unit in clusters of this size. Additionally, the difference in the cation:anion ratio on going from **2** to **6** was reflected in the microanalytical data obtained for both compounds. FAB mass spectra of **6** generated with silver salts gave no indication of a possible incorporation of silver into the metal core of the cluster. On exposure to light the brown-red solution of **6** in CH_2Cl_2 turns deep green, a process that is reversed after removal of the light source. The green cluster **7** has the same IR spectroscopic characteristics as **3** but with the set of three sharp infrared bands shifted in the same was as those of **6** with respect to **2**. If the green solution of **7** is exposed to moist air, the compound is immediately reduced to **3** with a concomitant change in color to burgundy red. On the other hand, oxidation of **3** with Ag^+ salts regenerates **7** quantitatively. FAB mass spectra of **7** showed the same molecular ion peak as those of **3** and gave no indication of a possible incorporation of silver into the metal core of the cluster. The anion **7** may therefore be formulated as $[Os_{18}Hg_2C_2(CO)_{42}]^-$, a formulation consistent with the microanalytical data obtained for its $[PPN]^+$ salt. Thus, the clusters **2**, **3**, **6**, and **7** are part of the reversible redox and photochemical cycle shown in Scheme I.

The Photolysis of $[PPN]_2[Os_{18}Hg_3C_2(CO)_{42}]$ (2). The clean photolytic conversion of **2** to the demercurated product **3** can be conveniently monitored by either UV–vis or IR spectroscopy as shown in Figure 5. The most significant change in the UV–vis spectrum is the decrease in intensity and bathochromic shift by 10 nm of the absorption band at 540 nm ($\epsilon = 4.38 \times 10^4$ L mol^{-1}

(15) Burlitch, J. M. In *Comprehensive Organometallic Chemistry*; Wilkinson, G., Stone, F. G. A., Abel, E. W., Eds.; Pergamon Press: New York, 1982; p 983.
(16) Vogler, A.; Kunkeley, H. *J. Organomet. Chem.* **1988**, *355*, 1.
(17) (a) Albinati, A.; Moor, A.; Pregosin, P. S.; Venanzi, L. M. *J. Am. Chem. Soc.* **1982**, *104*, 7672. (b) Ghilardi, C. A.; Midollini, S.; Moneti, S. *J. Chem. Soc., Chem. Commun.* **1981**, 865.
(18) Gade, L. H.; Johnson, B. F. G.; Lewis, J.; McPartlin, M. *J. Chem. Soc., Dalton Trans.* Submitted for publication.
(19) Gade, L. H.; Johnson, B. F. G.; Lewis, J. Unpublished results.

Scheme I. The Reversible Photochemical and Redox Chemical Cycle Linking **2**, **3**, **6**, and **7**[a]

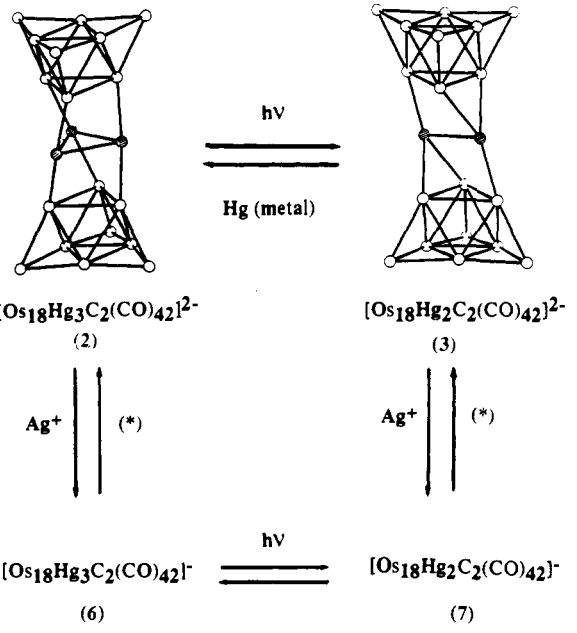

[a] The asterisk indicates standing in moist air.

Table VII. Quantum Yields for the Hg Extrusion of $[Os_{18}Hg_3C_2(CO)_{42}]^{2-}$ and $[Os_{18}Hg_3C_2(CO)_{42}]^-$ Complexes at 293 K

complex	λ_{ex}, nm	$10^3\Phi_{cr}$[a]
$[Os_{18}Hg_3C_2(CO)_{42}]^{2-}$ (**2**)	458	5.3
	488	5.1
	514	4.2
$[Os_{18}Hg_3C_2(CO)_{42}]^-$ (**6**)	458	4.6
	488	4.3
	514	3.6

[a] Reported values are in each case the mean of triplicate measurements.

cm^{-1}). Absorption bands in this energy range are due to metal–metal transitions within the cluster core. The high nuclearity of the system investigated and, consequently, the high density of electronic states prohibits a detailed analysis of the spectral features. However, since the structural changes that go along with the photochemical reaction are primarily confined to the mercury domain and its interfaces with the rest of the core, we believe that the intense absorption band which is so drastically affected in the process is at least partially due to metal-centered charge-transfer transitions to Os–Hg or Hg–Hg antibonding cluster valence orbitals. An additional feature is what appears to be an increase of the absorbance over the whole spectral range which is particularly marked at longer wavelengths. This is probably a consequence of light scattering by a suspension of colloidal mercury formed during the photolysis. The retention of sharp isosbestic points indicates that the photodemercuration proceeds without interference by secondary photoprocesses. This is confirmed by the sequence of IR spectra (Figure 5b) recorded after successive radiation intervals. The decrease in intensity of the ν(CO) infrared band at 2072 cm^{-1} and the growing in of the band at 2064 cm^{-1} are convenient indicators for the conversion of **2** to **3**.

Quantum yields of the reaction, Φ_{cr}, were obtained from the spectral sequences on successive irradiation with the 458-, 488-, and 514-nm lines of an Ar ion laser and are shown in Table VII. Within this spectral range they lie between 0.004 and 0.006 with a tendential increase toward the shorter wavelengths. Their low values are probably a consequence of the large number of nonreactive deactivation pathways for the cluster, but they may also reflect a highly efficient thermal back-reaction that regenerates the starting material during the period of photolysis.

If the photolysis is performed with UV light (337 nm, N_2 laser) the situation changes completely since metal to Os–CO (σ^*) transitions and consequent dissociation of carbonyl ligands compete with the demercuration reaction. This manifests itself in an increased degree of irregularity in the spectral sequence and consequent loss of sharp isosbestics, a problem that cannot be fully avoided by performing the experiment in a solution that was saturated with CO prior to the irradiation. In the presence of an excess of $P(OMe)_3$ (0.1 M in CH_2Cl_2) as a scavenging ligand the cluster degradation due to CO loss is suppressed, and the photolysis appears to progress as in the experiments with visible light, albeit with a quantum yield of $\Phi_{cr} = 2.8 \times 10^{-4}$, which is approximately one order of magnitude smaller. The Φ_{cr} obtained is to be interpreted as an effective value for what is probably a mixture of **2** and various in situ generated phosphite substituted derivatives. In order to be competitive with the radiationless decay of the Os–CO σ^* states to the lower lying metal centred states responsible for the Hg ejection, the Os–CO breaking reaction must take place rapidly. Indeed, the low quantum efficiency on UV excitation supports the notion that the upper excited state levels undergo efficient CO ligand extrusion, thereby reducing the extent of photochemical conversion to the metal centered levels which effect the Hg ejection; in other words, on UV photolysis most of the chemical reactions that occur are ligand substitutions.

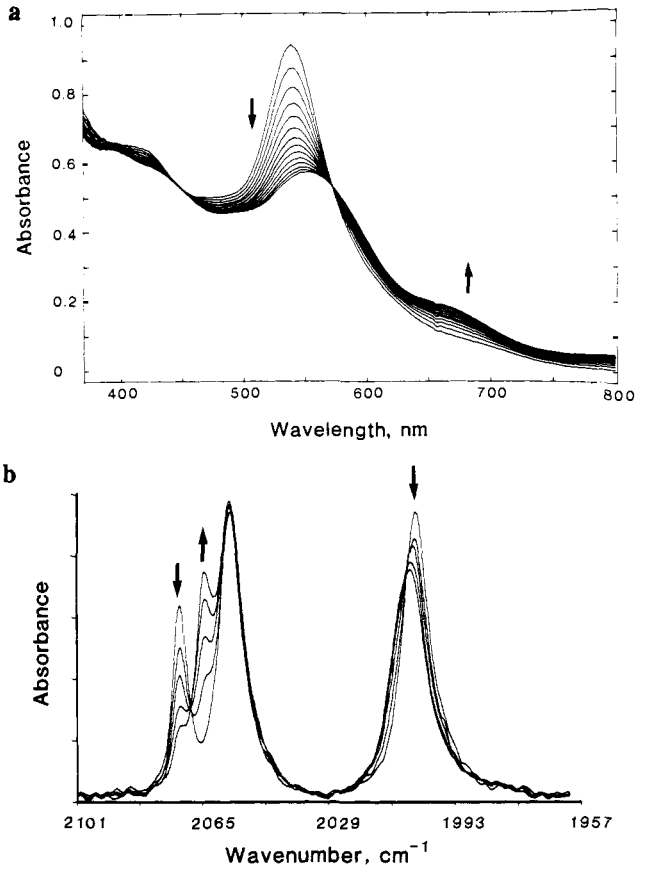

Figure 5. (a, top) UV–visible changes accompanying the 458-nm photolysis of 2.15×10^{-5} M $[PPN]_2[Os_{18}Hg_3C_2(CO)_{42}]$ (**2**) in deoxygenated CH_2Cl_2 at 293 K. Spectra were recorded at 30-s intervals. (b, bottom) Infrared spectral changes accompanying the 514-nm photolysis of **2**, in deoxygenated CH_2Cl_2 at 20 °C. Spectra were recorded at 120-s intervals.

In order to ensure that the scavenger did not interfere with the demercuration process, the photolyses at 458, 488, and 514 nm were repeated in the presence of 0.1 M $P(OMe)_3$. The quantum yields are identical within experimental error to those obtained earlier, which implies that the observed reaction is not affected by the phosphite.

The Photolysis of $[PPN][Os_{18}Hg_3C_2(CO)_{42}]$ (6). On oxidation of **2** with $Ag(O_2CCF_3)$ the dominant absorption band in the UV–vis spectrum is shifted from 540 to 526 nm, accompanied by a slight decrease in the extinction coefficient for this band from 4.38×10^4 to 4.04×10^4 L mol^{-1} cm^{-1}. The irradiation of solutions

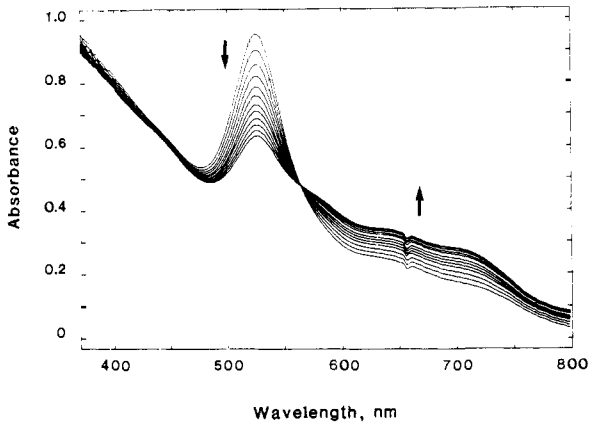

Figure 6. UV-visible changes accompanying the 458-nm photolysis of 2.35×10^{-5} M [PPN][$Os_{18}Hg_3C_2(CO)_{42}$] (**6**) in deoxygenated CH_2Cl_2 at 293 K. Spectra were recorded at 30-s intervals.

of the in situ generated monoanion **6** to generate **7** led to the complete disappearance of this band and the emergence of a weaker absorption band with its maximum at 570 nm. In the later stages of the photolytic conversion to the product the reaction occurred less cleanly than for the dianion **2**. The photolysis sequences, as e.g. shown in Figure 6, were therefore not carried through to the complete conversion of the starting material in the quantum yield determinations. The quantum yields for the three Ar ion laser lines lie between $\Phi_{cr} = 3.6 \times 10^{-3}$ and 4.6×10^{-3} (Table VII), i.e. slightly below those determined for **2**. Irradiation at 337 nm again led to a competition between metal-ligand dissociation processes and the demercuration, with an observed Φ_{cr} value of 2.0×10^{-4}. Since the oxidized cluster proved to be unstable in the presence of $P(OMe)_3$ and therefore analogous scavenging experiments were not feasible, this quantum yield value can only be regarded as a rough estimate of the photochemical demercuration process.

Conclusions

The aim of this study was the synthesis of systems and the development of methods which allow selective metal core transformations in large mixed-metal clusters. The cluster dianion $[Os_{18}Hg_3C_2(CO)_{42}]^{2-}$ has been shown to undergo photolytic demercuration to the corresponding dimercury cluster, a reaction that is thermally fully reversible and therefore provides the first example of photochromism in the chemistry of high-nuclearity clusters. The fact that this type of chemistry is feasible for two different oxidation states of the parent compound motivates further investigations into the redox and photochemistry of this and related systems. Such work is currently underway.

Acknowledgment. L.H.G. gratefully acknowledges the award of a Ph.D. scholarship by the Studienstiftung des deutschen Volkes and financial support by ICI Plc. M.McP. thanks the Science and Engineering Research Council (U.K.) for financial support, and A.J.L. thanks the donors of the Petroleum Research Fund, administered by the American Chemical Society, and the Division of Chemical Sciences, Office of Basic Energy Sciences, Office of Energy Research, U.S. Department of Energy (Grant DE-FG02-89ER14039), for support of this work. We are also grateful to Prof. M. E. Starzak (SUNY) for the use of the N_2 laser.

Supplementary Material Available: Tables of atomic coordinates and isotropic thermal parameters, anisotropic thermal parameters, and selected interbond angles (8 pages); listing of observed and calculated structure factors (25 pages). Ordering information is given on any current masthead page.

Synthesis and Characterization of the Mononuclear Compounds *t*-Bu_2MOAr (M = Al or Ga, Ar = Bulky Aryl Group): Are the Short Al-O and Ga-O Bonds a Consequence of π-Interactions?

Mark A. Petrie, Marilyn M. Olmstead, and Philip P. Power*

Contribution from the Department of Chemistry, University of California, Davis, California 95616. *Received May 17, 1991*

Abstract: The synthesis and characterization of the compounds *t*-Bu_2MOAr (Ar = 2,6-*t*-Bu_2-4-XC_6H_2, M = Al, and X = *t*-Bu, **1**; Me, **2**; H, **3**; X = Me and M = Ga, **4**) are described. They were characterized by X-ray crystallography (**1**, **2**, and **4**) and ^1H NMR and IR spectroscopy. In the crystal, the structures of **1**, **2**, and **4** are monomeric with essentially trigonal planar coordinations at the metals and short Al-O and Ga-O bond lengths that are near 1.71 and 1.82 Å. The structural data together with VT ^1H NMR studies indicate that there is probably little π-character in the M-O bonds. The shortness may be explained on the basis of an ionic bonding contribution and the low coordination number of the metal, with M-O π-interactions playing a relatively minor role. Crystal data with Mo Kα ($\lambda = 0.71069$ Å) at 130 K: **1**, $C_{26}H_{47}AlO$, $a = 11.386$ (10), $b = 29.11$ (2), $c = 24.969$ (16) Å, $\beta = 102.05$ (6)°, monoclinic, space group Pn, $Z = 12$ (six molecules per asymmetric unit), $R = 0.105$; **2**, $C_{23}H_{41}AlO$, $a = 8.200$ (2), $b = 17.876$ (4), $c = 15.910$ (4) Å, $\beta = 94.47$ (2)°, monoclinic, space group $P2_1/c$, $Z = 4$, $R = 0.047$; **4**, $C_{23}H_{41}GaO$, $a = 8.215$ (1), $b = 17.738$ (6), $c = 15.921$ (4) Å, $\beta = 94.73$ (2)°, monoclinic, space group $P2_1/c$, $Z = 4$, $R = 0.051$.

Introduction

The synthesis and structural characterization of compounds that have multiple bonding involving the heavier main group elements has been one of the major developments in inorganic/organometallic chemistry in recent years.[1] Much of this effort has concerned members of the phosphorus[2] or silicon groups.[3] The elements of the aluminum group have received much less attention in spite of the fact that their lighter congener boron is known to form multiple bonds to heavier main group elements such as sulfur,[4] phosphorus,[5] and arsenic[6] as illustrated.

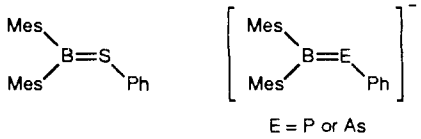

(1) For example, (a) Goldberg, D. E.; Harris, D. H.; Lappert, M. F.; Thomas, K. M. *J. Chem. Soc., Chem. Commun.* **1976**, *261* (Sn-Sn double bonds). (b) West, R.; Fink, M. J.; Michl, T. *Science (Washington, D.C.)* **1981**, *1343* (Si-Si double bonds). (c) Yoshifuji, M.; Shima, I.; Inamoto, N.; Hirotsu, K.; Higuchi, T. *J. Am. Chem. Soc.* **1981**, *103*, 4587 (P-P double bonds).

0002-7863/91/1513-8704$02.50/0